Synthesis, crystal structure and physical properties of $BaSnS_2$

Wilarachchige D. C. B. Gunatilleke[1], Andrew F. May[2], Angela R. Hight Walker[3], Adam J. Biacchi[3] and George S. Nolas[1*]

[1] *Department of Physics, University of South Florida, Tampa, FL, 33620, USA*

[2] *Materials Science and Technology Division, Oak Ridge National Laboratory, Oak Ridge, TN, 37831, USA*

[3] *Nanoscale Device Characterization Division, National Institute of Standards and Technology (NIST), Gaithersburg, MD 20899, USA*

ABSTRACT

Phase pure $BaSnS_2$, with space group $Pn2_1/c$, was synthesized and the structural and physical properties were investigated. The thermal properties and optical measurements are reported for the first time. The Debye temperature and Sommerfeld coefficient were obtained from temperature dependent heat capacity measurements, the latter indicating that $BaSnS_2$ is an electrical insulator. A direct band gap of 2.4 eV was obtained from diffuse reflectance and photoluminescence spectroscopy. The findings in this work lay the foundation for understanding the physical properties of this material, and are part of a continuing effort to investigate previously unexplored ternary chalcogenides.

Key words

Synthesis, Heat Capacity, Thermal Properties

* Email: gnolas@usf.edu

Metal chalcogenides continue to be investigated for diverse applications of interest including non-linear optics [1], thermoelectrics [2, 3], superconductivity [4] and ferroelectrics [5]. More recently, the synthesis and physical properties of ternary [6,7] and quaternary [8-11] chalcogenides have been of intense interest, not only due to an interest in their fundamental properties but also for applied research towards energy-related applications [12-16]. For certain materials the electrical properties can be modified by variation in stoichiometry [17-19], while others display transport properties that are atypical of compositions in this class of materials [20,21]. Certain compositions have also been synthesized in nanocrystalline form in order to investigate the effects of nano-structuring on the transport properties [22,23].

Many of the achievements outlined above have advanced our understanding of material formation and synthetic methodologies, as well as investigations into specific structure-property relationships that can now be realized by predictive computational and modelling methods [24]. Furthermore, chalcogenide compositions possess physical properties that are desirable for a variety of applications. Nevertheless, materials that are often seemingly simple to synthesize are, in fact, not readily obtained in phase-pure form, or have been reported in different structure types. One example of the latter case is $BaSnS_2$. It has been reported to form in different structure types, *e.g.*, $P2_1/c$ [25] and *Pnma* [26] although both reports describe very similar synthetic approaches. Moreover, to the best of our knowledge, the physical properties of this material have not been previously reported. Herein we report on the synthesis, thermal, and optical properties of $BaSnS_2$.

When employing the reported synthetic procedures phase pure $BaSnS_2$ was not obtained; therefore, substantial effort was involved in developing the synthetic procedure that is described below. Powder X-ray diffraction data for phase pure $BaSnS_2$ employing our synthetic approach are shown in Figure 1 and reveal the $P2_1/c$ crystal structure. This crystal structure, shown in Figure 2, can be thought of as a modified BaS rock salt structure with each of the Ba atoms bonded to six S atoms in an ideal octahedral geometry. In this way $BaSnS_2$ can be obtained if every other Ba atom in the crystal lattice was replaced by Sn, resulting in a distortion of the ideal octahedral geometry surrounding Ba due to the heterogeneous bonding to each of the Ba atoms. Although Sn is occupying an octahedral site in the structure, the Sn atoms are only bonded to three other S atoms

in a trigonal pyramidal local geometry. The $5s^2$ valence electrons form a lone pair to complete a tetrahedron that contains S atoms at the other vertices.

Figure 3 shows differential thermal analysis (DTA) data indicating that $BaSnS_2$ is thermally stable up to 925 K. Isobaric heat capacity, C_p, data are shown in Figure 4. The data approaches the Dulong-Petit limit at room temperature, an indication that the optic and acoustic mode frequencies are fully excited by this temperature. The Debye temperature, θ_D, can be calculated from the low temperature limit of the Debye model, $C_p = \gamma T + \beta T^3$, where γ is the Sommerfeld coefficient of the electronic contribution to C_p and β is the lattice contribution. The density of states at the Fermi level, $N(E_F)$, can be estimated from the relation [27],

$$\gamma = \frac{\pi^2}{3} k_B^2 N(E_F)\left(1 + \lambda_{e-ph}\right), \qquad (1)$$

where $\gamma = 0.04\ \mathrm{mJ\ mol^{-1}K^{-2}}$ from our data fit and λ_{e-ph} is the electron-phonon coupling constant, assumed to be zero as a first approximation, resulting in $N(E_F)$ = 0.04 eV^{-1} per formula unit. This basically null value is typical of electrical insulators. The inset in Figure 4(a) shows a fit to the low temperature data resulting in θ_D = 198 K by employing $\theta_D=(12\pi Rn/5\beta)^{1/3}$. Deviation from Debye-like behavior is observed at intermediate temperatures, as shown in Figure 4(b). From this figure, C_p/T^3 versus T shows a peak at low temperature indicating the influence of low-velocity optical modes. This peak can be associated with optic modes, at approximately 1/5 of the characteristic Einstein temperature, with an effective Einstein temperature of 59 K, the occurrence of which can be attributed to the preponderance of Einstein-like modes. Lone-pair electrons, required to form the trigonal pyramids in $BaSnS_2$, as well as trigonal bipyramidal local environments in the case of other chalcogenide materials, can be sources of low frequency modes [28-32]. Theoretical investigations on this material would be useful in elucidating further insight.

In order to further investigate the insulating behavior indicated by the low-temperature C_p data, diffuse reflectance and photoluminescence spectroscopy were employed. Diffuse reflectance data was collected on a film of $BaSnS_2$ powder starting in the near IR region and extending to the UV region. The absorption band edge was observed to begin at approximately 700 nm, as shown in Figure 5. A Tauc plot was constructed (inset in Figure 5) using the Kubelka-Munk transform of the diffuse reflectance plotted as a function of photon energy, $h\nu$ [33]. Linear fitting of the steepest

gradient provided an estimate of 2.4 eV for the photonic band gap. The good linear fit found with the square of the Kubelka-Munk function is indicative of a direct electron transition between the conduction and valence bands. The observation of a direct band gap was confirmed by photoluminescence spectroscopy, which detected broad visible light emission when excited with a 514.5 nm laser, peaking at 755 nm.

In conclusion, phase pure microcrystalline $BaSnS_2$ was synthesized. The ternary chalcogenide forms in a monoclinic crystal structure and is stable up to 925 K. Heat capacity data indicated θ_D = 198 K and contributions of Einstein-like optic modes at 59 K. The insulating behavior implied by the very small electronic contribution to heat capacity was confirmed by optical measurements and revealed a direct band gap of 2.4 eV. These results contribute towards the fundamental understanding of the physical properties of this material and will aid in the theoretical development of this as well as similar ternary chalcogenides.

EXPERIMENTAL SECTION

Attempts at synthesizing phase-pure specimens employing the appropriate binary compounds and procedures previously reported were unsuccessful. Adding excess S to the stoichiometric mixture also proved to produce other stable ternary phases. Additional phases $Ba_3Sn_2S_7$, $BaSn_3S_2$ and SnS were observed in all these attempted syntheses. Hence, we focused significant effort on investigating a synthetic approach that can produce phase-pure $BaSnS_2$. The synthesis method developed is as follows. High purity Ba pieces (Alfa Aesar, 99.9%), Sn powder (Alfa Aesar, 99. 85%) and ground S flakes (Alfa Aesar, 99.999%) were weighed in a 1:1:2 stoichiometric ratio inside a glovebox under a nitrogen atmosphere. The elements were mixed by hand before being loaded onto a quartz crucible and sealed in an evacuated silica ampoule. The elemental mixture was heated up to 1073 K at 15 K/hr and held at this temperature for 30 hr. The reaction mixture was cooled to 773 K at 2 K/hr, followed by cooling to room temperature at 10 K/hr. Powder X-ray diffraction data were obtained in Bragg-Bretano geometry using a Bruker D8 Focus Diffractometer, a graphite monochromator and CuKα (1.54056 Å) radiation. Differential thermal analysis (DTA) was performed with a TA Instruments Q600 apparatus. The isobaric heat capacity, *C*p, was measured from 1.8 K to 250 K using a commercial Quantum Design Physical Property

Measurement System (PPMS) with Apiezon N-grease and appropriate addenda. The maximum experimental error within the entire measured temperature range was ± 5%. UV-vis-NIR diffuse reflectance spectroscopy was performed with a PerkinElmer Lambda 950 equipped with a 150 mm integrating sphere. The band gap was determined using a Tauc plot of the Kubelka-Munk transform. Photoluminescence was collected using a Renishaw InVia with 514.5 nm Ar^+ laser excitation and emission detection on a 1'' CCD spread off a 1200 lines/mm grating. Certain commercial equipment, instrumentation, or materials are identified in this document to adequately specify the experimental procedures. Such identification does not imply recommendation or endorsement by the National Institute of Standards and Technology, nor does it imply that the products identified are necessarily the best available for the purpose.

ACKNOWLEDGEMENTS

This work was supported by National Science Foundation Grant No. DMR-1748188. Specific heat measurements (A.F.M.) were supported by the U.S. Department of Energy, Office of Science, Basic Energy Sciences, Materials Science and Engineering Division. Oak Ridge National Laboratory is managed by UT-Battelle LLC under contract DE-AC05000OR22725. A.J.B. and A.R.H.W. thank Catherine Cooksey (NIST) for use of instrumentation, and Joshua Martin and Dylan Kirsch (NIST) for their assistance with sample preparation.

REFERENCES

[1] I. Chung, M.G. Kanatzidis, *Chem. Mater.* **2016**, 26, 849.

[2] G.S. Nolas, J. Poon, M.G. Kanazidis, *MRS Bulletin* **2006**, 31, 199.

[3] Han, Chao, Qiao Sun, Zhen Li, and Shi Xue Dou, *Adv. Energy Mater.* **2016**, 6, 1600498.

[4] O. Fischer, *Solid-State Science*, Springer, Heidelberg, Germany, **1990**.

[5] R. V. Gamernyk, Y. P. Gnatenko, P. M. Bukivskij, P.A. Skubenko, V. Y. Slivka, *J. Phys.: Condens. Matter*, **2006**, 18, 5323.

[6] D. Aldakov, A. Lefrancois, P. Reiss, *J. Mater. Chem. C* **2013**, 1, 3756.

[7] G. R. Chen, C. H. Li, C. Y. Yu, M. F. Wang, C. S. Lee, *Inorg. Chem.* **2020**, 59, 11207.

[8] F-J. Fan, L. Wu, S. H. Yu, *Energy Environ. Sci.* **2014**, 7, 190.

[9] Y. Dong, A. R. Khabibullin, K. Wei, J. R. Salvador, G. S. Nolas, L. M. Woods, *Chem. Phys. Chem.* **2015**, 16, 3264.

[10] G. S. Nolas, S. M. Hassan, Y. Dong, J. Martin, *J. Solid State Chem*. **2016**, 242, 50.

[11] Guo, Z., Liu, Z., Deng, J., Lin, J., Zhang, Z., Han, X., Sun, F., Yuan, W., *J. Alloys Compd.*, **2021**, 160820.

[12] W. Shi, A. R. Khabibullin, D. Hobbis, G. S. Nolas, L. M. Woods, *J. Appl. Phys.* **2019**, 125, 155101.

[13] Y. Dong, H. Wang and G.S. Nolas, *Inorg. Chem.* **2013**, 52, 14364.

[14] D-J. Xue, B. Yang, Z-K. Yuan, G. Wang, X. Liu, Y. Zhou, L. Hu, D. Pan, S. Chen, J. Tang *Adv. Energy Mater.* **2015**, 5, 1501203.

[15] H. Lei, J. Chen, Z. Tan, Z., G. Fang, *Solar RRL* **2019**, 3, 1900026.

[16] M. R. Gao, Y. F. Xu, J. Jiang, S. H. Yu, *Chem. Soc. Rev.* **2013**, *42*, 2986.

[17] Y. Dong, H. Wang, G. S. Nolas, *Phys. Status Solidi RRL* **2014**, 8, 61.

[18] W. G. Zeier, A. LaLonde, Z. M. Gibbs, C. P. Heinrich, M. Panthöfer, G. J. Snyder, W. Tremel, *J. Am. Chem. Soc.* **2012**, 134, 7147.

[19] G. S. Nolas, H. Poddig, W. Shi, L. M. Woods, J. Martin, H. Wang, H., *J. Solid State Chem.* **2021**, 297, 122058.

[20] K. Wei, A. R. Khabibullin, T. Stedman, L. M. Woods, G. S. Nolas, *J. Appl. Phys.* **2017**, 122, 105109.

[21] K. Wei, G. S. Nolas, *ACS Appl. Mater. Interfaces* **2015**, 7, 9752.

[22] M. Ibáñez, R. Zamani, A. LaLonde, D. Cadavid, W. Li, A. Shavel, J. Arbiol, J. R. Morante, S. Gorsse, G. J. Snyder, A. Cabot, *J. Am. Chem. Soc*. **2012**, 134, 4060.

[23] C. Zhou, C. Dun, K. Wang, X. Zhang, Z. Shi, G. Liu, C. A. Hewitt, G. Qiao, D. L. Carroll, *Nano Energy*, **2016**, 30, 709.

[24] R. Gupta, N. Kumar, P. Kaur, C. Bera, *Phys. Chem. Chem. Phys.* **2020**, 22,18989.

[25] J.E. Iglesias, H. Steinfink, *Acta. Cryst.B* **1973**, 29 1480.

[26] M. Hervieu, G. Perez, P. Hagenmuller, *Bull. Soc. Chim. Fr.* **1967**, 6, 2189.

[27] C. Kittel, *Introduction to Solid State Physics*, John Wiley & Sons, New York, **1976**.

[28] W. Lai, Y. Wang, D. T. Morelli, X. Lu, *Adv. Funct. Mater.*, **2015**, 25, 3648.

[29] M. D. Nielsen, V. Ozolins, J. P. Heremans, 2013. *Energy Environ.*, **2013**, 6, 570.

[30] D. Hobbis, H. Wang, J. Martin, J., G. S. Nolas, *Phys. Status Solidi–Rapid Res. Lett.*, **2020**, 14, 2000166.

[31] Y. Dong, A. R. Khabibullin, K. Wei, J. R. Salvador, G. S. Nolas, L. M. Woods, *ChemPhysChem*, **2015** 16, 3264.

[32] A. R. Khabibullin, K. Wei,T. D. Huan, G. S. Nolas, L. M. Woods, *ChemPhysChem*, **2018** 19, 2635.

[33] P. Makuła, M. Pacia, W. Macyk, *J. Phys. Chem. Lett.* **2018** 9, 6814.

FIGURE CAPTIONS

Figure 1. Powder XRD data for $BaSnS_2$ (top) together with the calculated XRD pattern (bottom) for the monoclinic structure that crystallizes in space group $Pn2_1/c$.

Figure 2. Unit cell of $BaSnS_2$ with Ba (maroon), Sn (Grey) and S (yellow).

Figure 3. DTA data for $BaSnS_2$.

Figure 4. (a) Temperature dependent C_p for $BaSnS_2$ with the inset showing C_p/T vs T^2 data at low temperatures, where the solid line is a fit of the form $C_p/T = \gamma + \beta T^2$ and (b) C_p/T^3 vs T for $BaSnS_2$ illustrating deviation from Debye-like behaviour at low temperature.

Figure 5. UV-vis-NIR diffuse reflectance spectrum of $BaSnS_2$ with corresponding Tauc plot of the Kubelka-Munk function (inset), indicating a direct band gap of 2.4 eV.

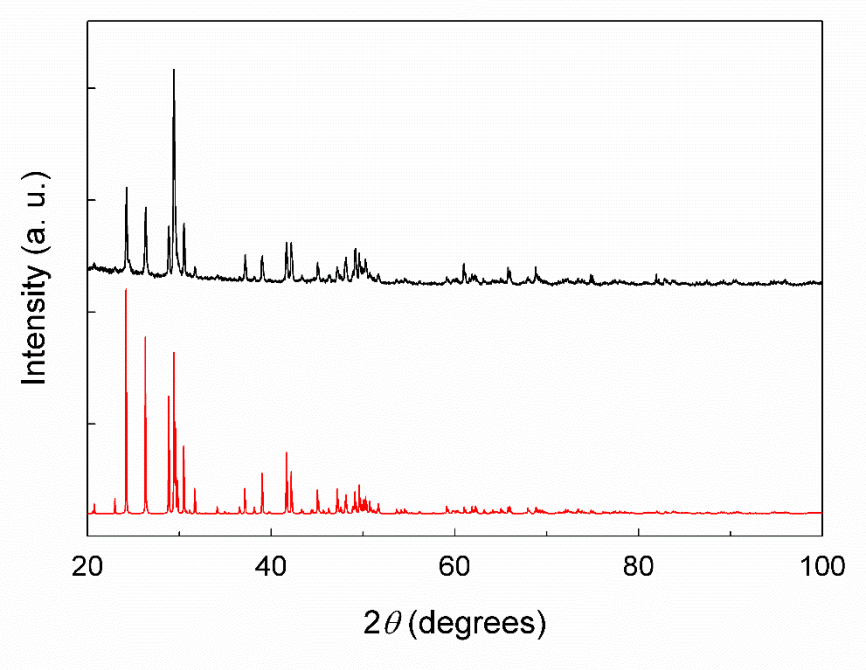

Figure 1

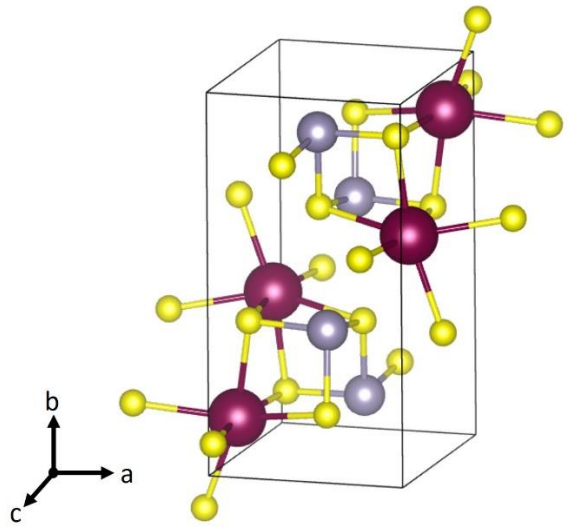

Figure 2

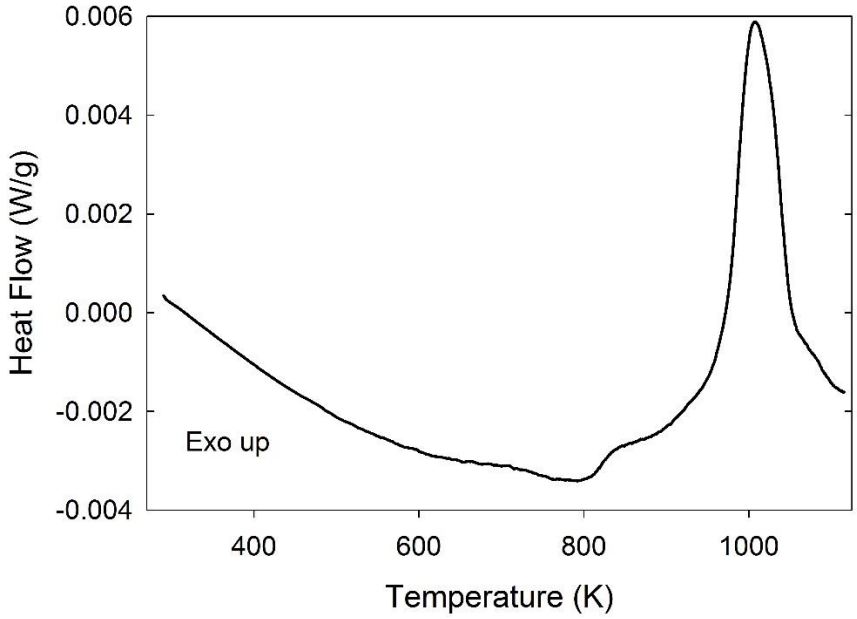
0.006
0.004
0.002
0.000
-0.002
-0.004
Heat Flow (W/g)
Exo up
400
600
800
1000
Temperature (K)

Figure 3

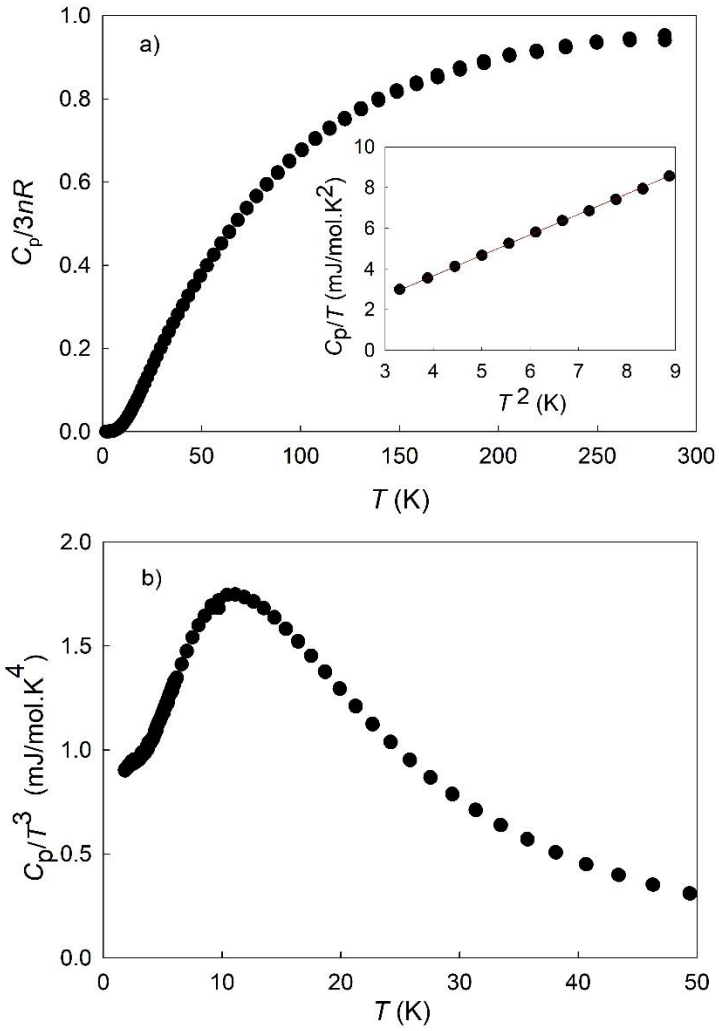

Figure 4

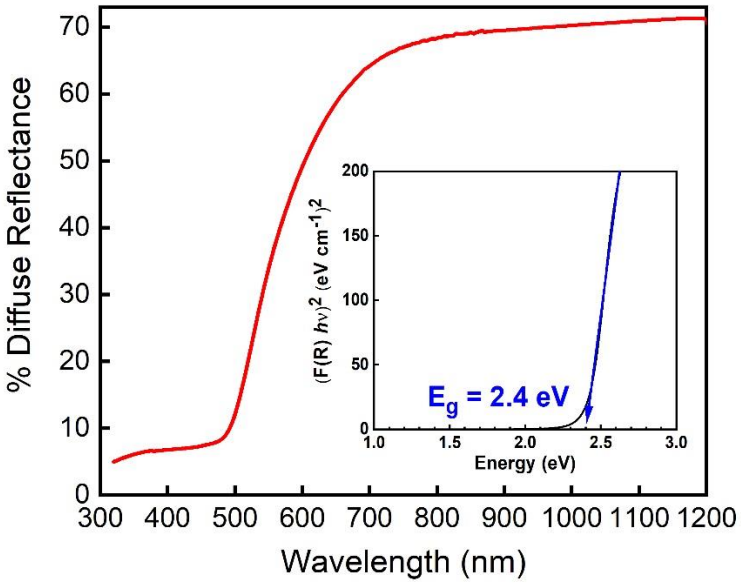
% Diffuse Reflectance
Wavelength (nm)
0
10
20
30
40
50
60
70
300
400
500
600
700
800
900
1000
1100
1200
(F(R) hν)2 (eV cm-1)2
Energy (eV)
Eg = 2.4 eV
0
50
100
150
200
1.0
1.5
2.0
2.5
3.0

Figure 5